

## Diagnostic Criteria for Choroidal Tumors Utilizing Optical Coherence Tomography (OCT) and Optical Coherence Tomography Angiography (OCTA) Findings: An Observational Study

Rehab Ismail<sup>1\*</sup>, Mohamed I Nowara<sup>2</sup>, Ahmed M Habib<sup>3</sup>, Hisham M Hassan<sup>3</sup>, Ihab A Mohamed<sup>3</sup>, Ashraf Soliman<sup>4</sup> and Ola M Ibrahim<sup>4</sup>

<sup>1</sup>Royal Victoria Infirmary, Newcastle, UK

<sup>2</sup>Electricity and Almashreq Eye Hospitals, Egypt

<sup>3</sup>Almashreq Eye Hospitals, Egypt

<sup>4</sup>Lecturer at Ophthalmology department, Ain Shams University, Egypt

\*Corresponding Author: Rehab Ismail, Royal Victoria Infirmary, Newcastle, UK.

Received: June 08, 2020; Published: July 31, 2020

### Abstract

**Introduction:** Well established pathognomonic Optical Coherence Tomography (OCT) and Optical Coherence Tomography Angiography (OCTA) findings for choroidal tumors are lacking.

**Purpose:** To evaluate spectral domain OCT SD-OCT using choroidal enhancement technique (EDI) and more recently OCTA in detecting diagnostic criteria of choroidal tumors

**Methods:** A multicenter observational study was conducted between 2007 and 2017 for recently diagnosed choroidal tumors using OCT and OCTA technology.

Qualitative analysis included the overlying retina, tumor surface and internal features, light penetration within the mass (intra lesion reflectivity) by OCT, and surrounding blood vessel changes by OCTA, in addition to discrimination from surrounding choroidal tissue.

**Results:** A total of 50 eyes were identified and included for analysis. These were clinically classified into: choroidal metastasis, choroidal hemangioma, choroidal melanoma, choroidal nevus.

SD-OCT identified precise criteria for each tumor type, and distinguished tumor landmarks from the surrounding normal choroid. OCTA highlighted various changes to the surrounding and overlying blood vessels and was performed on a total of 12 eyes.

**Conclusion:** SD-OCT and OCTA are efficient in detecting pathognomonic criteria for different types of choroidal tumors and can be used as a non-invasive diagnostic tools.

**Keywords:** OCT; Choroidal Tumors; Choroidal Metastasis; Choroidal Nevus; Choroidal Hemangioma; Choroidal Melanoma; EDI; Choroidal Enhancement Technique

### Introduction

Choroidal tumors are the most common intraocular tumors with severe impact on vision. There are various types including melanocytic nevi, melanomas, metastases, cavernous hemangioma and other less common tumors as lymphoma, neurilemmoma, leiomyoma and osteoma. Indirect ophthalmoscopy, fundus photography, and ultrasonography remain the main methods of diagnosis [1].

Other ancillary tests such as fundus fluorescein angiography (FFA) and Optical Coherence Tomography (OCT) and Optical Coherence Tomography Angiography (OCTA) can be helpful in differentiating the various types of tumors by drawing up a set of diagnostic criteria for each tumor type.

OCT has been widely accepted by ophthalmologists worldwide as an efficient ocular modality providing wealth of information on retinal conditions. It uses a wavelength of around 800 nm. A significant portion of this wavelength is reflected by the retinal pigment epithelium (RPE). Therefore, OCT imaging of choroidal tumors has been challenged by its limited penetration into the choroid secondary to the light scattering from the RPE [2]. The use of a wavelength of 1050 nm (swept-source OCT) can provide more penetration into the choroid and better resolution of images. With the evolution of OCT machines with shorter acquisition times and enhanced resolution, better quality images could be taken of choroidal lesions but applicability is still limited to the overlying retina and lesion surface [3].

Spaide and coauthors described two techniques for image acquisition of choroidal lesions improving image resolution and depth down to the level of the sclera [5]. The first technique is the choroidal enhancement technique (CET) in which the objective lens is moved further towards the eye so that the acquired image becomes inverted showing the choroid in a better way. The second technique is the enhanced depth imaging (EDI) which is the same technique but done automatically by the machine producing an upright image with normal orientation. This allows thickness measurement and reflective quality of small (< 3 mm) choroidal masses such as choroidal nevus and melanoma [3,4]. With these techniques, high-resolution deeper images of the choroid and sclera can be obtained enabling better analysis of the surface as well as the surrounding choroid [5].

Some of the previous attempts to study choroidal tumors using non-EDI spectral and time domain OCT techniques have only visualized the anterior aspect of tumors with non-specific intrinsic reflectivity patterns [1]. They used these OCT findings for detection and follow up of the signs of activity of choroidal tumors [9,10].

There are gaps in knowledge on the applicability of OCT and OCTA in the diagnosis of choroidal lesions and tumors [5]. This gap in knowledge needs to be addressed to help diagnosis of choroidal tumors without subjecting patients to invasive investigations.

Our team has therefore conducted an observational descriptive study aiming to establish consistent SD-OCT and OCTA elicited diagnostic criteria for various choroidal tumors, providing a reliable non-invasive differentiating tool.

## **Methods**

Our team has conducted a multicenter observational study on choroidal tumors over ten-year period to identify the diagnostic criteria using the imaging technology OCT. OCTA was performed on patients diagnosed with choroidal tumors over the last two years of the study, when the machine was introduced into one of the contributing centers.

Our research team has led a multicenter study between 2007 and 2017 in three centers in Cairo, Egypt. Only patients meeting the enrolment criteria were included in the analysis. OCT images were taken at the time of their initial diagnosis.

The aims, safety, and efficacy of the imaging procedures were explained to the participants before enrolment and an informed consent was obtained from each patient. All investigators adhered to the ethical standards of Good Clinical Practice.

## **Inclusion criteria**

- Patients with recently diagnosed choroidal tumors without any previous intervention.
- Documented diagnosis of choroidal tumors by a diagnostic tool other than OCT.
- Clear media.
- Tumor location posterior enough for the OCT machine to acquire acceptable images.
- Tumor size small enough for the OCT machine to be able to detect the anterior edge with the overlying retina.

### Image analysis

- Identification of the choroidal lesion, overlying retinal changes (retinal edema, retinal thinning, photoreceptor layer loss or thinning), retinal pigment epithelium (RPE)/choriocapillaris findings (RPE/choriocapillaris thickening, RPE/choriocapillaris hyper-reflectivity, RPE/choriocapillaris fragmentation, RPE/choriocapillaris surface irregularity). Other image analyses include tumor surface reflectivity (anterior choroidal reflectivity), choroidal pattern, surrounding choroid and intra-lesion penetration depth, underlying shadowing and reflectivity (hyporeflective, isoreflective and hyperreflective).
- OCTA findings were limited to 12 eyes as this technology was introduced into one of the centers in late 2015. The analysis of OCTA included vessel caliber (compressed, dilated) and wall regularity, arrangement of the vessels, and search for feeders. Lack of signal or signal void in OCTA was attributed to either too slow or too fast flow (compressed lumens), luminal invasion, or shadowing from the tumor itself (such as in melanomas and metastasis).

### Results

Fifty eyes of 48 patients were included in the analysis and classified into the following groups (n = 18 males, n = 30 females): choroidal metastasis (n = 17 eyes), choroidal hemangioma (n = 8 eyes), choroidal melanoma (n = 7 eyes) (n = 5 eyes melanotic and n = 2 eyes amelanotic variant), choroidal nevi (n = 18) (n = 16 eyes melanotic variant and n = 2 eyes amelanotic variant). In all eyes, spectral domain OCT was able to clearly distinguish choroidal tumor tissue from the surrounding healthy choroid and neighbouring structures. Adjacent structures of choroidal melanoma of more than 1 mm thickness (4 eyes) could not be scanned (out of the field). However, the junction between normal and abnormal structure could be scanned as well as imaging the tumor surface n = (2 eyes).

### Choroidal metastases

Choroidal metastases (n = 17) demonstrated one or more of the signs of activity within the overlying retina surface explicitly subretinal fluid (SRF) (n = 17), intraretinal fluid (IRF) (n = 9), subretinal exudation (SRE) (n = 8.5) and subretinal fibrosis. Eight eyes showed lobulated surface (Figure 1), while 2 eyes had very small tumors with a single lobule in a patient with metastasising breast carcinoma. All scans revealed loss of the choroidal pattern within the lesion with fair intralesional light reflectivity (intralesional penetration depth).

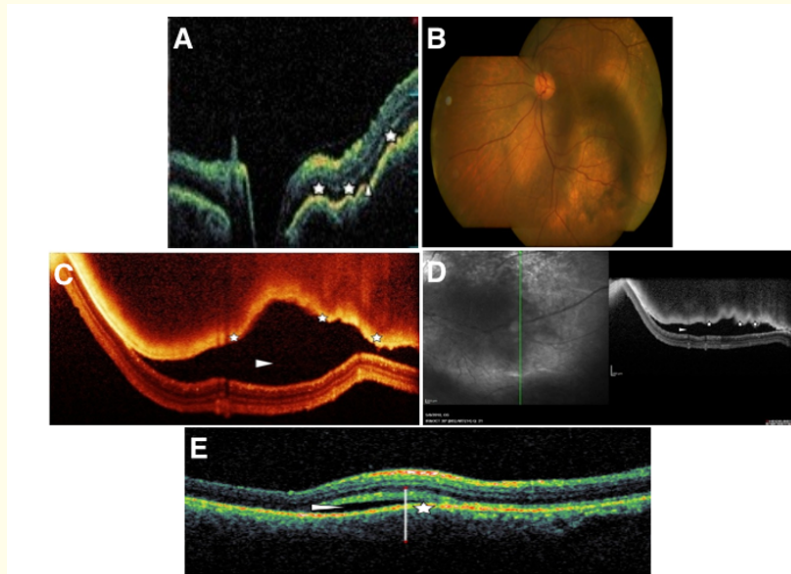
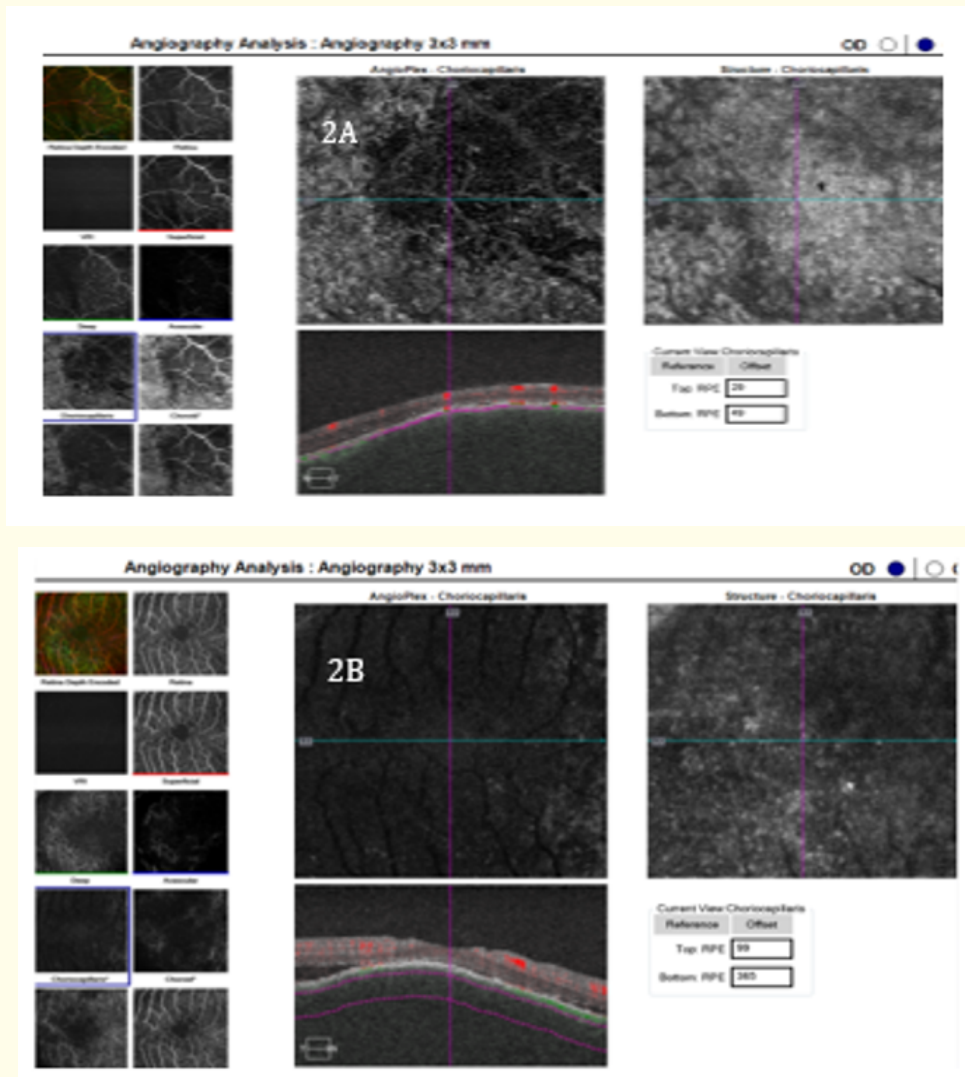


**Figure 1:** Choroidal metastatic lesion with lobulated surface (stars) and subretinal fluid (arrow head). It presents as a single elevation (E) in early stages or in small masses.

OCTA was done on three patients in this group (Figure 2). Findings revealed loss of the normal mottled choriocapillaris and choroidal pattern, within the choriocapillaris and deep choroidal slabs respectively. A large area of flow void “signal void” corresponding to the tumor area was observed and suggestive of metastatic invasion of the vascular lumen of vessels in the affected area.

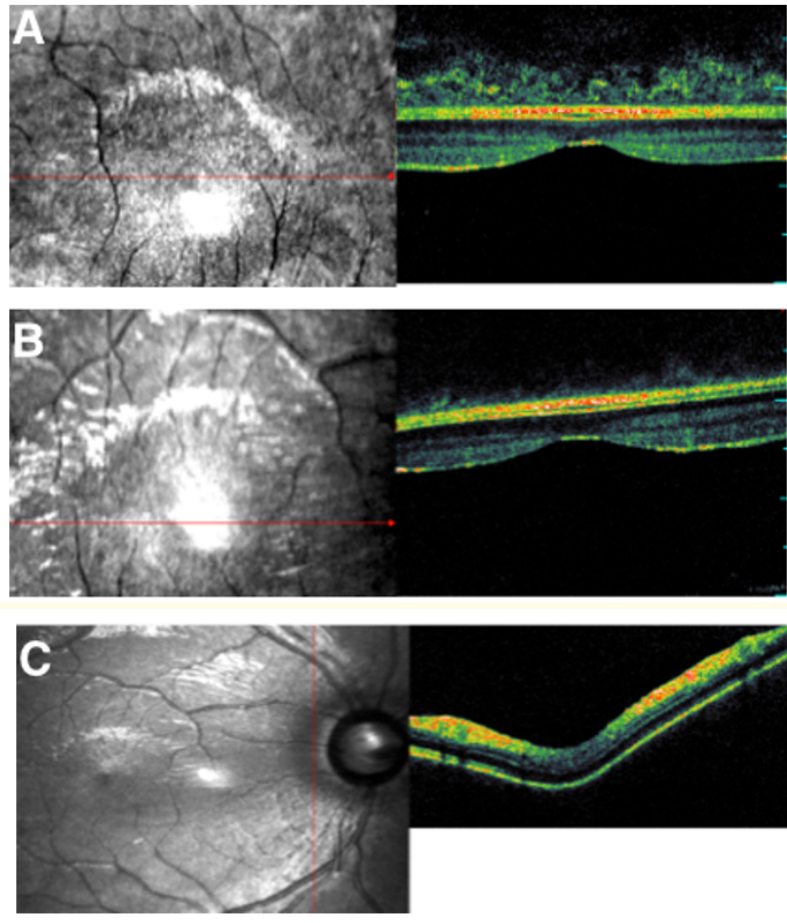


**Figures 2a and 2b:** OCTA of a patient with choroidal metastases from a breast carcinoma. Figure 2a is the choriocapillaris slab which shows loss of the normal mottled appearance, and a corresponding area of signal void in the deep choroidal slab. Figure 2b: loss of signal from within the vessels is suggestive of tumor invasion of blood vessel lumen.

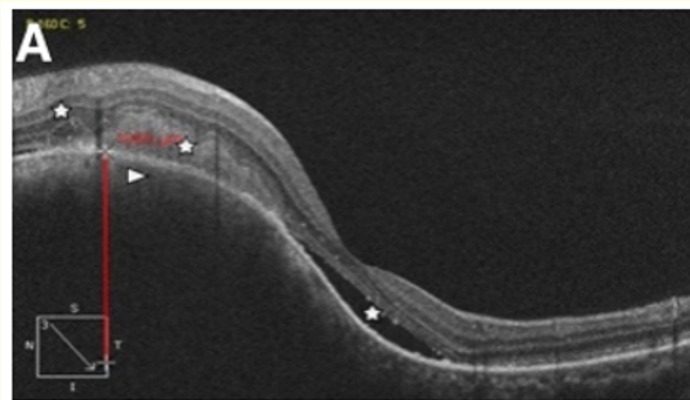
### Choroidal hemangioma

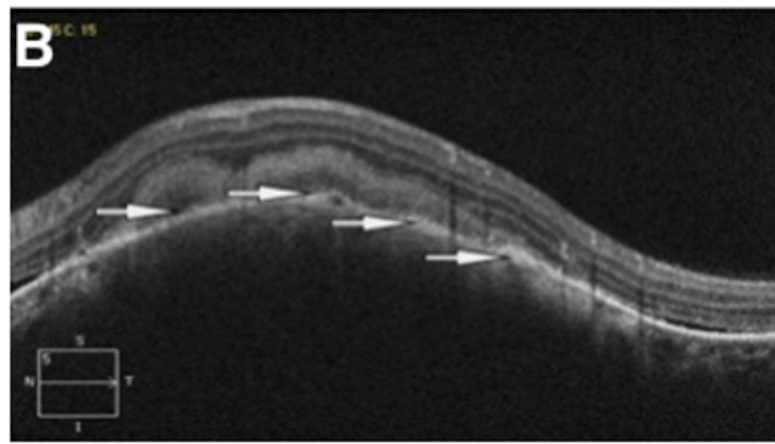
In the choroidal hemangioma group (n = 8) (Figure 3 and 4), seven eyes demonstrated signs of activity within the overlying retina, e.g. SRF (n = 6), IRE (n = 4) one of which showed schisis-like changes, SRE (n = 4) and subretinal fibrosis (n = 2).

Only one eye did not demonstrate signs of activity and it was a diffuse hemangioma in a clinically quiescent stage. The seven eyes with activity had a mamillated surface as seen below in figure 4A and 4B, while the single patient in the quiescent stage showed smooth



**Figure 3:** A thin layer of interrupted Hyperreflectivity (arrow head) in a normal eye (A). Diffuse hemangioma (B) with absence of choroidal pattern and elevation at the edge of the disc (C).

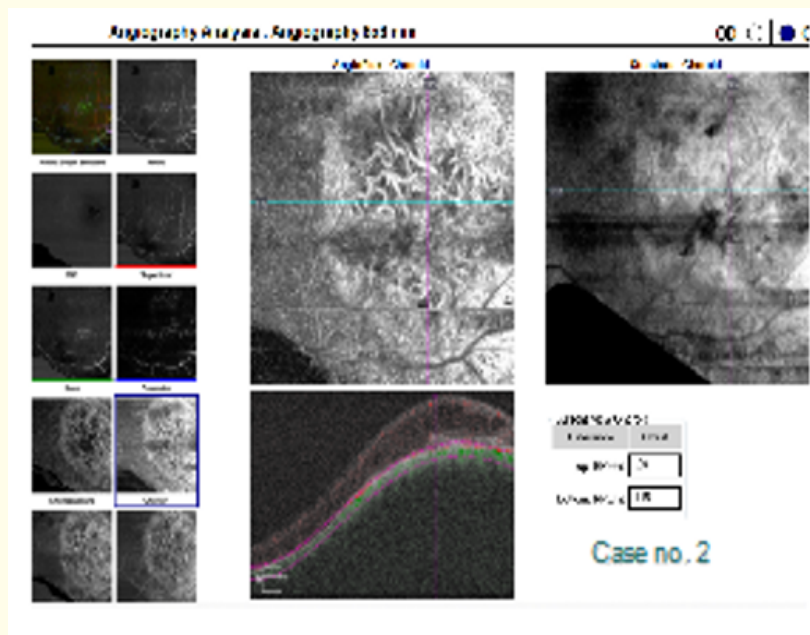


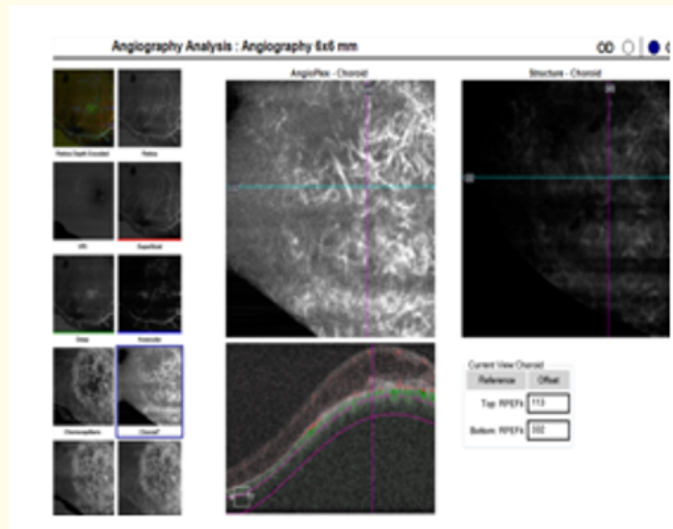


**Figure 4:** Localized hemangioma presenting as a dome-shaped mass with mammillated surface (arrows), loss of choroidal pattern, and low penetration of coherent light and low to medium interrupted hyperreflectivity (arrow head) and signs of activity (stars).

surface. All patients demonstrated loss of choroidal pattern with poor intralesional reflectivity and with a band of moderate reflectivity with intrinsic spaces only near the surface.

OCTA was performed on two eyes only (Figure 5a and 5b). Findings revealed loss of the normal choriocapillaris and choroidal pattern within each level slab, and the presence of an abnormally large branching and anastomosing vascular network within the choriocapillaris and choroidal slabs, which could be easily distinguished from the surrounding normal choroidal pattern.

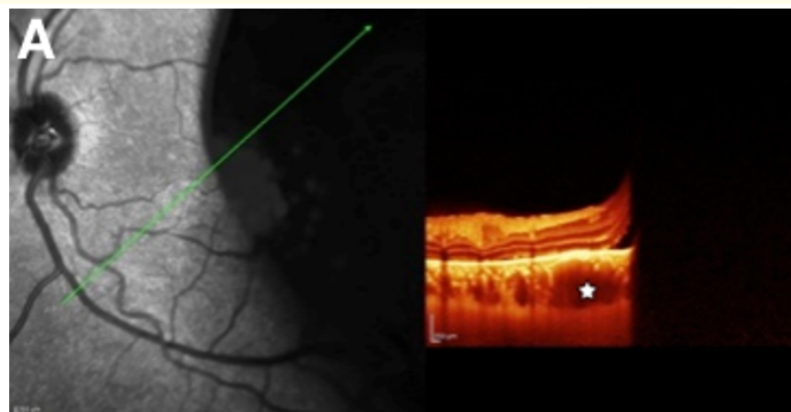


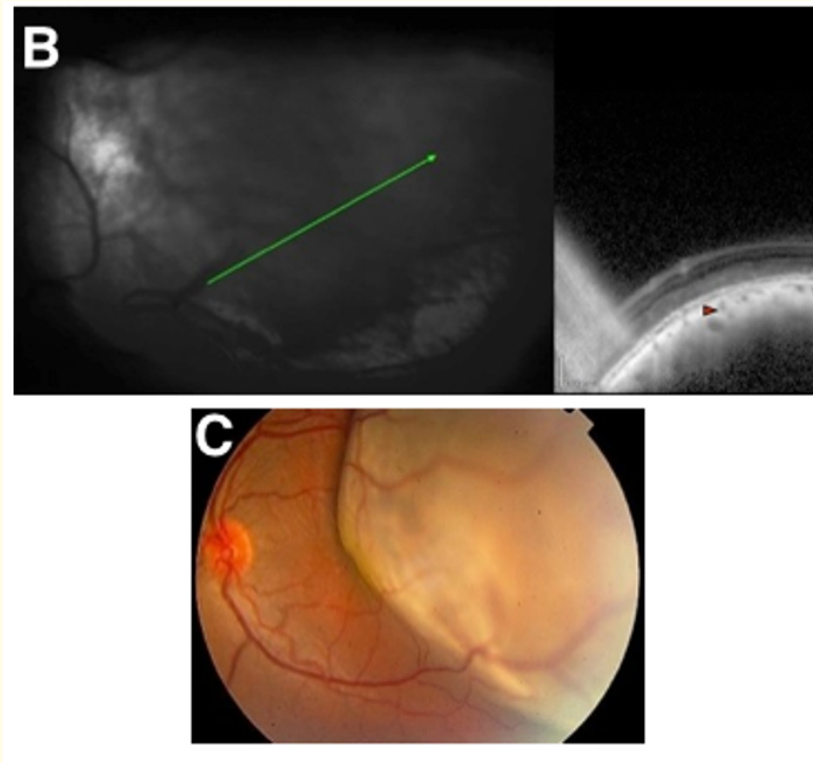


**Figure 5a and 5b:** OCTA of a choroidal hemangioma which demonstrates loss of the normal appearance in both choriocapillaris (5a) and deep choroidal (5b) slabs, and the presence of an easily distinguishable network of arborizing vessels, representing the hemangioma itself.

### Choroidal melanoma

Eyes with choroidal melanoma (n = 7) demonstrated large dome-shaped surface that could not be detected with adjacent retina in the same scan, due to tumor height. All eyes demonstrated SRF and loss of the normal choroidal pattern. The 5 eyes with melanotic melanoma demonstrated poor intralesional reflectivity with homogenous hyperreflective band near the surface. The 2 eyes with amelanotic melanoma (Figure 6) demonstrated IRE and SRF, in addition to enlargement and coalescence of the large choroidal vessels at the adjacent edge of the tumor denoting choroidal congestion. The site of the lesion itself demonstrated good intralesional reflectivity (tightly compacted tumor cells) with multiple variable sized, ellipsoid hyporeflective spaces. Unfortunately, due to the time taken for OCTA image acquisition, the scans taken for melanomas were of very poor quality, since the technology depends on ocular stability, and in addition to tumor height the image could not be captured at the same site.

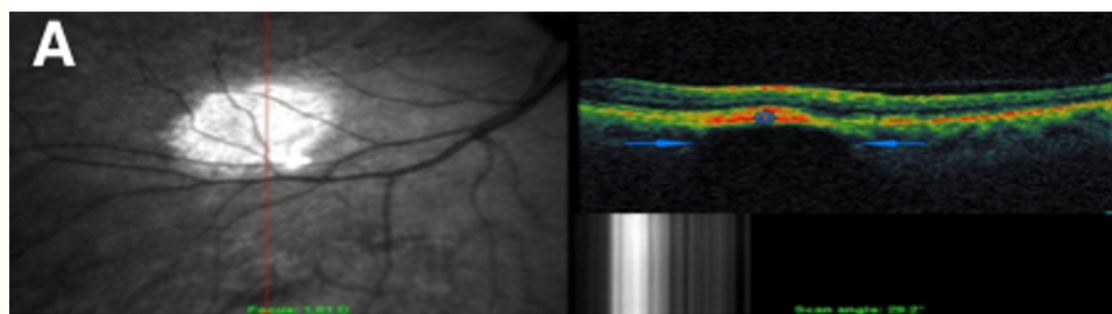




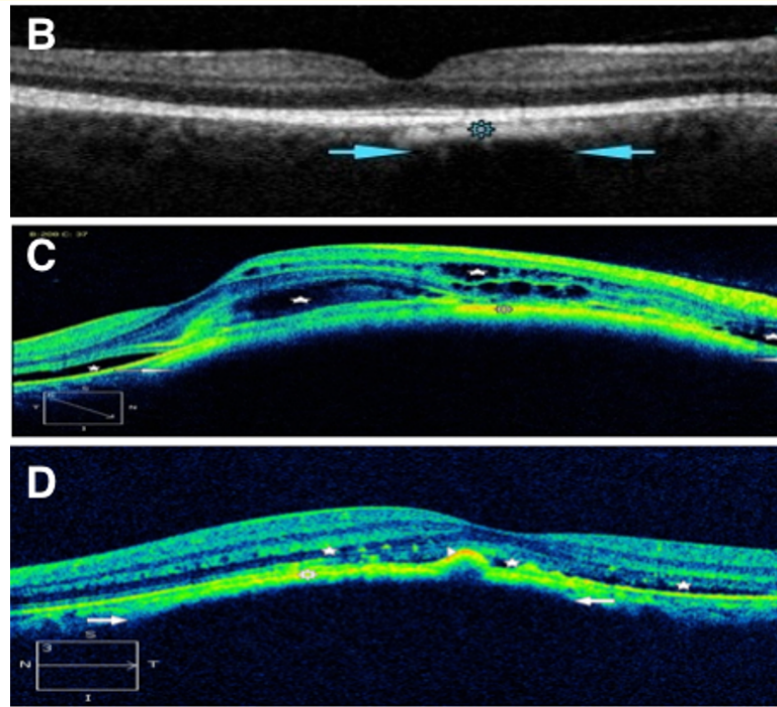
**Figure 6:** Amelanotic melanoma presenting as a single dome-shaped mass with smooth surface and deep penetration of the coherent light. Note the dilated blood vessels at the tumor edge, and compressed vessels on top of the tumor (arrow head) by Spectralis EDI (A, B).

### Choroidal nevi

Eighteen eyes with choroidal nevi, the melanotic variant (Figure 7) (n = 16) demonstrated minimally elevated surfaces and loss of the underlying choroidal pattern. In addition, there was poor intralaminar reflectivity with a hyperreflective band near the surface shadowing the underlying structures.

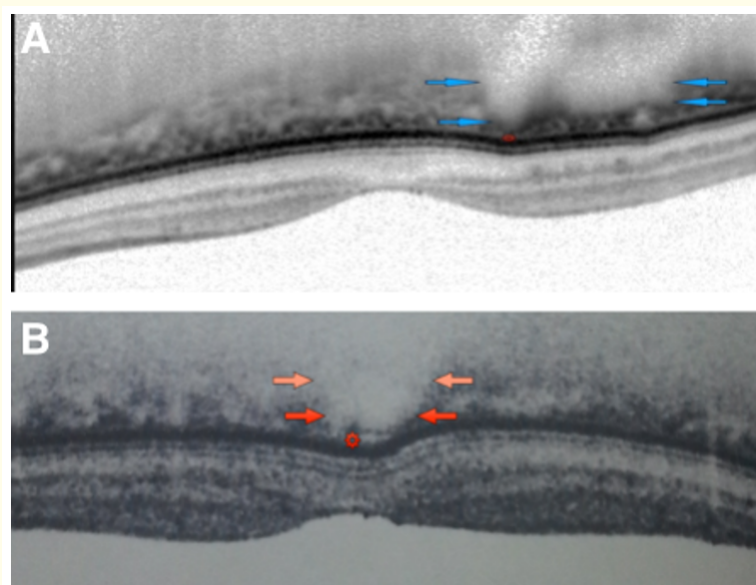






**Figure 7:** Melanotic nevus (arrows) with overlying hyperreflective band resembling RPE and underlying it (gear) with shadowing below. Suspicious nevus (C) with signs of activity (star). Nevus (D) with overlying drusen (arrow head).

Equally, amelanotic nevi (n = 2) demonstrated good intralesional reflectivity with a moderately reflective band not shadowing the underlying structures (Figure 8).



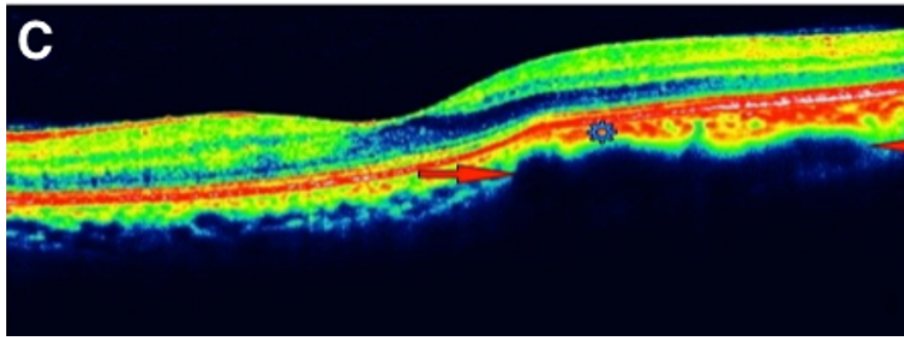


**Figure 8:** Amelanotic nevus presenting within the large choroidal vessels (arrows) with overlying compressed choroidal vessels (gear).

Sixteen of eighteen eyes with choroidal nevi demonstrated normal overlying retina. The remaining 2 eyes demonstrated suspicious nevi displaying signs of activity. Both eyes had sub-retinal fluid, hyper-reflective deposits and drusen, whereas only one of them showed intraretinal edema (Table 1 and 2).

Pathology	Overlying retina	Surface of the lesion	Underlying choroid	Intralesional light penetration	Discrimination
Choroidal metastasis (n = 17 eyes)	SRF (n = 17,100%), IRE (n = 9,60%) SRE (n = 8.5,50%)	Lobulated (n = 15, 80%) Single nodule (n = 2, 20%)	Lost (n = 17, 100%)	100% 17/17 Deep (n = 17, 100%)	Identified (n = 17, 100%)
Choroidal Hemangioma (n = 8 eyes)	SRF (n = 6, 75%), IRE (n = 4,50%), SRE (n = 4, 50%), Subretinal fibrosis and schisis (n = 2, 25%)	Mamillated (n = 6, 85.7%) (6/6 of circumscribed lesions)	Lost (n = 8, 100%)	Limited to the surface with intrinsic hyporeflective spaces (n = 8, 100%)	Identified (n = 8, 100%)
Choroidal melanoma (n = 7 eyes)	SRF (n = 7 100%), IRE (n = 5.5, 78.5%), SRE (n = 3.5, 50%)	7/7 large dome-shaped 100%	Lost (n = 7, 100%)	No penetration in melanotic and deep penetration in amelanotic	not identified (n = 7,100%)
Choroidal Nevus (n = 18 eyes)	Normal quiescent nevi (n = 16, 88.8%) Suspicious nevi with signs of activity (n = 2, 11.1%)	Hyper-reflective band of elevation (n = 18, 100%)	Lost (n = 18, 100%)	No penetration (n = 16, 75%)	Identified (n = 18, 100%)

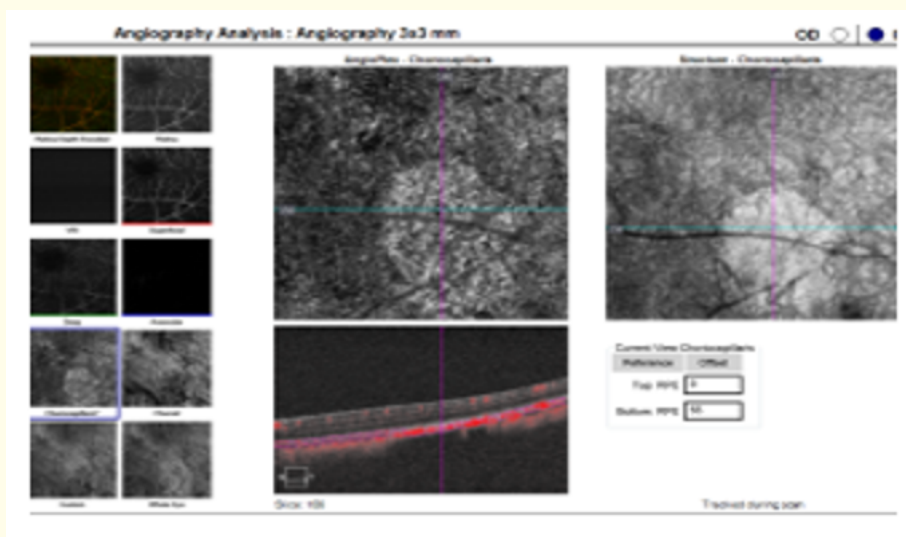
**Table 1:** Grouped results (percentages of findings).

**Abbreviations:** SRF: Sub-Retinal Fluid; IRE: Intraretinal Edema; SRE: Sub-Retinal Exudation.

Pathognomonic criteria	Choroidal melanomas	Suspicious Choroidal Nevi	Choroidal Metastases	Choroidal Hemangiomas
Sub-retinal fluid	+	+	+	+
Lesion surface	Large domed shaped	Hyper reflective elevated band	Early stages: small single elevation that shows multiple small lobulations Advanced cases: multi lobulated surface	Mammillated
Intra-lesional penetration of light	No penetration		Deep with fair intralesional reflectivity	Limited to the surface with intrinsic hypo-reflective spaces
Loss of the choroidal pattern	+	+	+	+
OCTA	2 cases attempted and failed	Significant mottled hyper reflectivity within the choriocapillaris slab overlying the nevus, probably due to vascular compression Choroidal slab shows signal void corresponding to the en face image suggestive of shadowing	Loss of normal choriocapillaris and deep choroidal vessels, signal void corresponding to tumor area indicative of metastatic luminal invasion	Loss of normal mottled choriocapillaris and large choroidal vessels Presence of an abnormally large branching anastomosing network of blood vessels easily distinguished from the normal vasculature

**Table 2:** Suggested OCT and OCTA criteria for the assessment of choroidal tumors.

OCTA findings of the melanotic choroidal nevi (Figure 9a and 9b) included significant mottled hyper reflectivity within the choriocapillaris slab overlying the nevus, most probably due to vascular compression. While the choroidal slab demonstrated an area of signal void corresponding to the en face image, suggestive of shadowing.



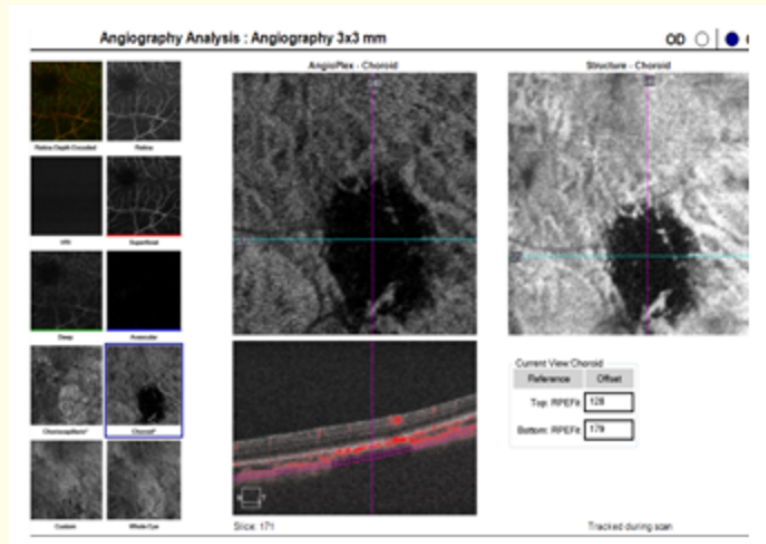


**Figure 9a and 9b:** OCTA of melanotic nevus showing mottled hyperreflectivity in the choriocapillaris layer suggestive of vascular compression, and congruent loss of signal in the deep choroidal plexus indicative of shadowing from the melanin in the superficial layers.

OCTA 2 cases attempted and failed Significant mottled hyper reflectivity within the choriocapillaris slab overlying the nevus, probably due to vascular compression.

Choroidal slab shows signal void corresponding to the en face image suggestive of shadowing Loss of normal choriocapillaris and deep choroidal vessels, signal void corresponding to tumor area indicative of metastatic luminal invasion Loss of normal mottled choriocapillaris and large choroidal vessels Presence of an abnormally large branching anastomosing network of blood vessels easily distinguished from the normal vasculature.

## Discussion

Our team has identified diagnostic criteria for choroidal tumors using the new modalities OCT and OCTA.

Our team has identified a total of fifty eyes (18 males, 30 females) and included in the analysis. The research team has identified precise criteria for each tumor type, using SD-OCT and distinguished tumor landmarks from the surrounding normal choroid. In addition, various changes to the surrounding and overlying blood vessels have been highlighted using OCTA.

Our findings were classified as characteristics relevant to lesion surface, intra-lesional penetration of light and loss of choroidal pattern.

As regards lesion surface, we identified findings as follows: a) choroidal melanomas: demonstrate large domed shaped surface; b) choroidal nevi: hyper reflective elevated band; c) choroidal metastasis: Early stages: reveal small single elevation that shows multiple small lobulations; whereas Advanced cases: reveal multi lobulated surface; d) choroidal hemangiomas: acquire mamillated surface.

With regards to intra-lesional penetration of light: a) choroidal melanomas: demonstrate no penetration; b) choroidal metastasis: display deep with fair intralesional reflectivity; c) choroidal hemangiomas: were limited to the surface with intrinsic hypo-reflective spaces. Loss of choroidal pattern were displayed by all tumors.

Our work identified that small choroidal metastasis (n = 2) showed a small choroidal elevation with minimal overlying SRF and hyper-reflective subretinal substance. The remaining 15 eyes showed a single mass with multi-lobulated surface allowing good light penetration and moderate reflectivity of the optical coherent beam. In addition, there was loss of the normal internal appearance of the choroid, and presence of one or more retinal abnormalities as retinal edema, cystic changes, SRF, subretinal exudation and pigment epithelial detachment. Thirteen eyes received external beam radiation; which upon follow up, led to the resolution of subretinal fluid, intraretinal edema and smoothing of the anterior surface with reappearance of normal choroidal pattern. We found a large area of signal void in the choriocapillaris and deep choroidal vessels corresponding to the tumor area.

On the other hand, Luliano and coworkers described SD-OCT characteristics in a case of bilateral choroidal metastasis scanned at different stages [14]. They described marked irregularity of the RPE with thickening and gross undulation. They also described another lesion in the other eye of the same patient, which was at an earlier stage, smaller in size and comprised of a single dome shaped mass with subretinal fluid and hyper-reflective subretinal spots representing the early stage of the choroidal metastasis [15]. Similar features were found in our early stage patient.

In our study, choroidal nevi demonstrated similar features that were comparable to those described by Torres' work [7], with the exception of the amelanotic nevus which displayed good intralésional reflectivity with a moderately reflective band not shadowing the underlying structures. In addition to the previously mentioned features, these tumor cases also demonstrated apparent compression of the large choroidal vessels between the RPE and the nevus tissue. This feature was also seen in the amelanotic choroidal melanoma along with the other features of activity.

In a study conducted by Shields and co-workers, they drew up a few intrinsic features for choroidal nevi. They found a gradual transition between the hyper reflective inner choroid and the hypo reflective outer choroid, with loss of the choriocapillaris over the bulk of the nevus, and widespread undulations of the overlying RPE suggestive of drusen. They were also able to investigate the reflectivity of the anterior surface of the choroid (hypo, iso, hyper reflective) depending on the amount of pigment within the tumor and the overlying RPE atrophy; these OCT findings portrayed the pigment within the mass and did not correspond to the inter reflectivity and acoustic quality by b scan which depends mainly on cellular density and compactness [13].

In our study, choroidal hemangiomas revealed a mamillated surface and demonstrated loss of choroidal pattern with poor intralésional reflectivity and a band of moderate reflectivity with intrinsic spaces only near the surface.

Liu and coworkers examined 14 cases with circumscribed lesions receiving photodynamic therapy using time domain OCT, and described SRF, intraretinal edema and localized photoreceptor loss in some of their cases [9]. Torres and coauthors examined 3 cases with circumscribed choroidal hemangioma using the EDI SD-OCT technique and described medium to low reflective band without shadowing [16]. Ramasubramanian and colleagues described OCT findings in choroidal hemangioma and found subretinal fluid (19%), retinal edema (42%), retinal schisis (12%), macular edema (24%), and localized photoreceptor loss (35%). They described the tumor as a dome shaped mass with a hyporeflective anterior surface [9].

### **Strengths and Weaknesses of the Study**

This was a multicenter study conducted over 10 year period and incorporated advancing technology in diagnosing and classifying choroidal tumors.

A limitation of our study was our inability to fully scan the entire depth of choroidal melanoma lesions because they usually exceed 3 mm in thickness, which is beyond the scope of the OCT beam penetration. Another limitation was lack of histopathologic evidence of diagnosis since most of the affected eyes were not enucleated. Nevertheless, two eyes that had large amelanotic melanomas had undergone enucleation and histopathological examination, which confirmed the initial diagnosis.

### **Meaning of the Study: Implications for Clinicians and Policymakers**

This observational study demonstrated feasibility of directly imaging a variety of frequently encountered benign and malignant choroidal tumors with SD-OCT EDI technique and OCTA. This can be particularly useful in detection of small choroidal tumors such as choroidal nevi that are undetectable by ultrasonography. Development of Choroidal enhancement technique/Enhancement depth image used in this study was useful in obtaining deeper images of choroidal tumors and defining specific features with characteristic changes for each. OCTA can be coupled with EDI to further assess these conditions and define their vascular details. We believe that these criteria can help early diagnosis of life threatening conditions in a timely manner without the need of invasive procedures.

### **Conclusion**

SD-OCT using EDI and OCTA are efficient in differentiating various types of choroidal tumors, and can be used as auxiliary non-invasive diagnostic tools. Currently, no OCT findings are pathognomonic for a specific tumor. Our study has identified specific qualitative SD-OCT features for a variety of commonly encountered benign and malignant choroidal tumors.

### **Acknowledgement**

We would like to thank staff members at Al Mashreq eye hospitals, Cairo, Egypt for their constant support and diligent effort in putting this work together.

We would also like to thank Professors Emad ElSawy and Mohamed Alkady for helping us in this manuscript, in addition to the nursing staff at Ain Shams Specialized hospital, Cairo, Egypt.

### **Conflicts of Interest and Source of Funding**

The authors declare no conflict or commercial interests.

### **Bibliography**

1. Sayanagi K., *et al.* "3D Spectral domain optical coherence tomography findings in choroidal tumors". *European Journal of Ophthalmology* 21 (2011): 271-275.
2. Singh AD., *et al.* "Fourier domain optical coherence tomographic and auto-fluorescence findings in indeterminate choroidal melanocytic lesions". *British Journal of Ophthalmology* 94 (2010): 474-478.
3. Say EA., *et al.* "Optical Coherence Tomography of Retinal and Choroidal Tumors". *Review Article Journal of Ophthalmology* (2011): 12.
4. Copete S., *et al.* "Direct comparison of spectral-domain and swept-source OCT in the measurement of choroidal thickness in normal eyes". *British Journal of Ophthalmology* 98 (2014): 334-338.
5. Spaide RF., *et al.* "Enhanced depth imaging spectral-domain optical coherence tomography". *American Journal of Ophthalmology* 146 (2008): 496-500.
6. Matsunaga D., *et al.* "OCT Angiography in Healthy Human Subjects". *Ophthalmic Surgery, Lasers and Imaging Retina* 45.6 (2014): 510-515.
7. De Carlo TE., *et al.* "A review of optical coherence tomography angiography (OCTA)". *International Journal of Retina and Vitreous* 1 (2015): 5.
8. Arevalo JF., *et al.* "Optical Coherence Tomography Characteristics of Choroidal Metastasis". *Ophthalmology* 112 (2005): 1612-1619.
9. A Ramasubramanian., *et al.* "Autofluorescence of choroidal hemangioma in 34 consecutive eyes". *Retina* 30.1 (2010): 16-22.

10. MA Blasi, *et al.* "Photodynamic therapy with verteporfin for symptomatic circumscribed choroidal hemangioma: five-year outcomes". *Ophthalmology* 117 (2010): 1630-1637.
11. CL Shields, *et al.* "Optical coherence tomography of choroidal nevus in 120 patients". *Retina* 25.3 (2005): 243-252.
12. Shah SU, *et al.* "Enhanced depth imaging optical coherence tomography of choroidal nevus in 104 cases". *Ophthalmology* 119 (2012): 1066-1072.
13. Shields CL, *et al.* "Review of optical coherence tomography for intraocular tumors". *Current Opinion in Ophthalmology* 16 (2005): 141-154.
14. Torres VLL, *et al.* "Optical Coherence Tomography Enhanced Depth Imaging of Choroidal Tumors". *American Journal of Ophthalmology* 151 (2011): 586-593.
15. Luliano L, *et al.* "SD-OCT patterns of the different stages of choroidal metastases". *Ophthalmic Surgery, Lasers and Imaging Retina* (2012): 43.
16. Liu W, *et al.* "Optical coherence tomography for evaluation of photodynamic therapy in symptomatic circumscribed choroidal hemangioma". *Retina* 31 (2011): 336-343.
17. Cennamo G, *et al.* "Evaluation of choroidal tumors with optical coherence tomography: enhanced depth imaging and OCT-angiography features". *Eye* 31.6 (2017): 906-915.

**Volume 11 Issue 8 August 2020**

**©All rights reserved by Rehab Ismail, *et al.***